Signalling-competent truncated forms of ErbB2 in breast cancer cells: differential regulation by protein kinase C and phosphatidylinositol 3-kinase

Azucena ESPARÍS-OGANDO, Elena DÍAZ-RODRÍGUEZ and Atanasio PANDIELLA[1]

Instituto de Microbiología Bioquímica, Consejo Superior de Investigaciones Científicas-Universidad de Salamanca, Avenida del Campo Charro s/n, 37007 Salamanca, Spain

Alterations that affect the ectodomain of receptor tyrosine kinases are often associated with constitutive activation of the enzymic activity of the mutant cell-associated receptor. Since the ectodomain of the ErbB2 receptor tyrosine kinase has been detected as a soluble fragment in the culture supernatant of cells and serum from patients with advanced breast cancer, the possible presence of cell-associated truncated forms of ErbB2 in cancer cells was investigated. Several cell-bound N-terminal truncated forms of ErbB2 were identified in breast cancer cells over-expressing this receptor. The presence of the truncated fragments was independent of lysosomal/proteasomal activity, indicating that classical receptor tyrosine kinase degradation systems were not involved in the N-terminal cleavages. The presence of these truncated forms of ErbB2 was up-regulated by protein kinase C and neuregulin; and down-regulated by phosphatidylinositol 3-kinase, and monoclonal antibodies that target the ectodomain of ErbB2, indicating that N-terminal cleavages of ErbB2 were regulated by multiple mechanisms. The truncated fragments were tyrosine-phosphorylated under resting conditions, and associated with the signalling intermediates Shc and Grb2. It is therefore likely that these truncated forms may be endowed with constitutive activity that allows them to permanently signal.

Key words: cleavage, proteases, signalling.

INTRODUCTION

Receptor tyrosine kinases of the ErbB family play essential roles in several physiological processes such as cell growth [1–3], differentiation and tissue development [4–6]; and have been implicated in pathological processes, such as tumour generation and/or progression [2,3]. This family comprises four structurally related transmembrane receptors, the epidermal growth factor receptor (EGFR), ErbB2, ErbB3 and ErbB4, that bind a large repertoire of epidermal growth factor-like ligands [1].

The ectodomain of these receptors has been recovered as a soluble fragment from the culture supernatant of cells or animal fluids. The mechanisms involved in the generation of these soluble forms include genetic [7–12] and proteolytic mechanisms [13–17]. Aberrant transcripts of the EGFR are responsible for the production of soluble forms of the ectodomain in A431 carcinoma cells [8]. In this cell line, the EGFR is amplified and rearranged, and translocation of the 5′ region of the EGFR gene results in the production of a 2.8 kb transcript whose translation produces a soluble EGFR ligand-binding domain [8]. In the adult chicken liver [9] and human placenta [10], alternative splicing of the EGFR mRNA gives rise to receptor transcripts that code for truncated forms of the EGFR that are secreted. Functionally, the released soluble forms are able to interact with EGFR ligands [18] and may thus act as a buffering system that prevents ligand-induced receptor activation [9,18]. Soluble forms of ErbB3, generated by alternative splicing, have also been reported in the MNK45 gastric cancer cell line [11].

A soluble form of ErbB (sErbB4) is also detected in the culture media of cells that express this receptor [19–21]. The mechanism for the generation of sErbB4 involves proteolytic cleavage rather than genetic mechanisms. The ErbB4 receptor has been shown to be cleaved in an extracellular juxtamembrane position resulting in the shedding of its ectodomain, and this is accompanied by the accumulation of an 80-kDa cell-bound receptor fragment that contains the transmembrane and tyrosine kinase domains [19]. Cleavage of ErbB4 may be up-regulated by treatments such as protein kinase C (PKC) activation [19] or tyrosine phosphatase inhibition [21], which affect the phosphorylation status of cellular proteins. Even though these treatments appear to act by different pathways [21], the high sensitivity of the cleavage of ErbB4 to hydroxamic-acid-based protease inhibitors indicates that multiple pathways converge into a common final metalloprotease-dependent proteolytic system [21]. Functionally, the cleavage of ErbB4 may have several implications that are related to the biological roles of the resulting two receptor fragments. On one side, removal of the ligand-binding ectodomain decreases the number of cell-surface receptors available for ligand-induced stimulation, and in this respect cleavage may act as a down-regulation mechanism [19]. On the other side, cleavage generates cell-associated receptor fragments whose signalling activity may be higher than the resting parental holoreceptors. In fact, the truncated cell-bound fragment of ErbB4 is tyrosine phosphorylated, and in the absence of any exogenously added ligand the phosphotyrosine content of the truncated fragment appears to be higher than that of the unstimulated holoreceptor [20]. Furthermore, the truncated fragment of ErbB4 has been found to constitutively bind signalling molecules such as Shc and phospholipase C-γ [19].

The soluble ectodomain of ErbB2 has also been detected in the culture supernatant of cancer cells [13,14,16,17] and the body fluids of patients with advanced cancer [15]. Direct evidence of a

Abbreviations used: ALLN, *N*-Ac-Leu-Leu-norleucinal; BIM, bisindolyl maleimide; DMEM, Dulbecco's modified Eagle's medium; EGFR, epidermal growth factor receptor; GST, glutathione S-transferase; HRP, horseradish peroxidase; KRH, Krebs–Ringer Hepes; mAb, monoclonal antibody; MA, mitogen-activated protein kinase; MEK, MAPK kinase; NHS-LC, succinimidyl-6-(biotinamido)hexanoate; NRG, neuregulin; PI3K, phosphatidylinositol 3-kinase; PKC, protein kinase C; sErbB, soluble form of ErbB; TAPI-2, *N*-{D,L-[2-(hydroxyaminocarbonyl)methyl]-4-methylpentanoyl}-L-3-(2′-naphthyl)-alanyl-L-alanine 2-aminoethylamide; TPCK, tosylphenylalanylchloromethyl ketone.

[1] To whom correspondence should be addressed (e-mail atanasio@gugu.usal.es).

role for this receptor in ligand buffering is, however, lacking due to the fact that no ligand with high-affinity binding to ErbB2 has been isolated [22]. However, sErbB2 has been reported to counteract the inhibitory effect that an antibody directed to the ErbB2 ectodomain has on the growth of breast cancer cells [7]. The production of sErbB2 has been attributed to both proteolytic processing and alternative transcripts [7,17]. Evidence for the former as the mechanism of ErbB2 solubilization has been obtained from pulse–chase experiments [14] and immunoprecipitation of sErbB2 from the culture media of surface-labelled SKBR3 cells [15]. In addition, treatment with certain protease inhibitors has been reported to decrease the production of sErbB2 in this cell line [15]. An alternative transcript coding for the ErbB2 ectodomain has also been reported in SKBR3 cells [7] and the expression of the cDNA corresponding to this transcript in COS-1 cells resulted in the production of a secreted, as well as intracellular, ErbB2 ectodomain [7].

The reverse correlation between a good prognosis in cancer patients overexpressing ErbB2 and the presence of a soluble form of this receptor in the serum of these patients [15], together with the finding that truncated cell-associated forms of receptor tyrosine kinases may have increased constitutive activity [19,23], prompted us to investigate whether a regulated cleavage analogous to the one that participates in ErbB4 cleavage was responsible for the solubilization of the ectodomain of ErbB2, and to search for the presence of truncated signalling-competent forms of ErbB2 in cell lines overexpressing this receptor. While investigating the mechanism of generation of the soluble forms of the ErbB2 receptor, we noticed that the ectodomain of this receptor was cleaved at the N-terminal portion rather than in an extracellular juxtamembrane region. Cleavage at the N-terminus of ErbB2 generated cell-bound truncated forms of this receptor, and the system responsible for such cleavage was found to be controlled by different intracellular signalling pathways that affect the phosphorylation status of cellular proteins. The truncated forms of ErbB2 were found to associate with signalling molecules such as Shc and Grb2, indicating that these cleaved forms may be biologically active.

MATERIALS AND METHODS

Reagents and immunochemicals

The monoclonal anti-ErbB2 ectodomain antibody 4D5 and neuregulin (NRG) α were provided by Dr Mark X. Sliwkowski (Genentech, San Francisco, CA, U.S.A.). The Ab-3 and Ab-2 monoclonal anti-ErbB2 endodomain antibodies and the Ab-1 polyclonal anti-ectodomain antibody were from Oncogene Science (Uniondale, NY, U.S.A.). The polyclonal M6 anti-ErbB2 antiserum was from Dr Matthias Kraus (Istituto Europeo di Oncologia, Milan, Italy). An anti-endodomain polyclonal antiserum towards the EGFR was raised in rabbits injected with a glutathione S-transferase (GST)–EGFR fusion protein (see below). The monoclonal antibody (mAb) 528, directed against the ectodomain of the human EGFR, was generously provided by Dr John Mendelsohn (Memorial Sloan Kettering Cancer Center, New York, U.S.A.). The anti-phosphotyrosine mAb 4G10 and the anti-Shc antiserum were from UBI (Lake Placid, NY, U.S.A.) and the anti-PKC antibodies from Transduction Laboratories. GSH–Sepharose and Protein A–Sepharose were from Pharmacia. PVDF blotting membranes were from Millipore. Secondary antibodies to rabbit and mouse, and Protein A–peroxidase were from Bio-Rad. PMA, wortmannin, LY294002, cycloheximide, chloroquine, trypsin (sequencing grade), protease inhibitors and other generic chemicals were obtained from Sigma or Boehringer Mannheim. TAPI-2 (*N*-{D,L-[2-(hydroxyaminocarbonyl)methyl]-4-methylpentanoyl}-L-3-(2′-naphthyl)-alanyl-L-alanine 2-aminoethylamide) was provided by Dr Roy Black (Immunex, Seattle, WA, U.S.A.). NHS-LC-biotin [succinimidyl-6-(biotinamido)-hexanoate] was from Pierce. Rapamycin, bisindololyl maleimide (BIM), Gö6983, and PD98059 were from Calbiochem. [γ-^{32}P]ATP was from Amersham.

Cell culture and transfections

All cells were cultured at 37 °C in a humidified atmosphere in CO_2/air (1:19, by vol.). Cells were grown in DMEM containing high glucose (4500 mg/l) and antibiotics (penicillin 100 units/ml, streptomycin 100 μg/ml) and supplemented with 5% (CHO cells) or 10% (v/v) (rest of the cell lines) fetal-bovine serum.

The cDNA coding for ErbB2 (provided by Dr M. Kraus) was subcloned into the pCDNA3 vector (Invitrogen) and transfected into CHO cells by the calcium phosphate technique [24]. Colonies resistant to G418 were selected and tested for expression by FACS using the 4D5 mAb.

Fusion proteins for antibody generation and ErbB2 precipitation

A fusion protein that corresponded to the 301 C-terminal residues of the human EGFR was produced in bacteria using standard protocols [24]. In brief, a *Bam*HI–*Xho*I fragment of the EGFR was subcloned into identical cloning sites of the pKG vector [25]. Transformed bacteria with this construct were induced with 0.2 mM IPTG for 2 h at 37 °C. Bacteria were lysed and GST–EGFR isolated from the lysate by GSH–Sepharose affinity chromatography. The fusion protein was eluted from the resin with reduced GSH and the amount of protein was quantified by SDS/PAGE using various amounts of BSA as standard. Portions of the fusion protein (100 μg) were used for the primary immunization of rabbits, followed by boosts with 50 μg. Antisera were collected and tested by Western-blotting using A431 cell lysates as controls.

The GST–Grb2 fusion protein was produced following an analogous protocol. The vector, which included full-length Grb2 (generously provided by Dr Piero Crespo, University of Cantabria, Santander, Spain), was introduced into *Escherichia coli* and bacterial cells were induced and lysed as above. An aliquot of the fusion protein coupled to GSH–Sepharose was separated by SDS/PAGE gel to quantify the amount of the fusion protein. The fusion protein (10 μg) coupled to the GSH–Sepharose resin were used for the precipitation of ErbB2 and related fragments from 2 mg of SKBR3 lysates. After extensive washing of the beads with immunoprecipitation lysis buffer, and bound material was subjected to SDS/PAGE on 6% acrylamide gels. Blots were probed with the Ab-3 antibody as described below.

Metabolic labelling, immunoprecipitations, Western blotting and gel-overlay experiments

SKBR3 or BT474 cells were washed twice, 15 min each, with methionine- and cysteine-free DMEM, and incubated in this medium supplemented with 500 μCi/ml of a mixture of [^{35}S]methionine and [^{35}S]cysteine for times that ranged from 4–16 h. Monolayers were washed twice, 15 min each, with DMEM and chased with or without PMA. Media samples were collected and immunoprecipitated with the anti-ectodomain antibody 4D5, and cell lysates were immunoprecipitated with either Ab-3 or 4D5 antibodies. The resulting immunoprecipitates were resolved by SDS/PAGE (6 or 8% gels), and bands were detected by autoradiography. Where indicated, the intensity of the bands was quantified with a PhosphorImager.

For immunoprecipitation, cells were washed once with cold PBS and lysed in 0.5–1 ml of ice-cold lysis buffer (140 mM NaCl, 10 mM EDTA, 10% (v/v) glycerol, 1% (v/v) Nonidet P-40, 20 mM Tris/HCl, pH 8.0, 1 mM PMSF, 1 mM sodium orthovanadate). After scraping the cells from the dishes, samples were centrifuged at 10000 ***g*** for 10 min, and the supernatants were transferred to new tubes with the corresponding antibody and Protein A–Sepharose. Immunoprecipitations were performed for 2 h at 4 °C and immune complexes were recovered by a short centrifugation, followed by three washes with 1 ml of cold lysis buffer. Samples were then boiled in electrophoresis sample buffer and resolved by SDS/PAGE (6 or 8% gels). The resolved proteins were transferred to PVDF membranes, the filters were blocked for 1 h in blocking buffer (140 mM NaCl, 10 mM Tris/HCl, pH 7.5, 0.05% (v/v) Tween 20, and 1% (w/v) BSA) and then incubated for $\geqslant$ 1 h with the corresponding antibody. After extensive washing, the membranes were incubated with horseradish peroxidase (HRP)-coupled secondary antibodies or Protein A. Bands were visualized by a luminol-based detection system with *p*-iodophenol enhancement [23].

For surface immunoprecipitation, cells pre-treated for 4 h with or without PMA were incubated with 1 μg of the 4D5 anti-ectodomain antibody for 2 h at 4 °C, washed twice with PBS and lysed. After removal of cell debris, Protein A–Sepharose was added, and after a 30 min incubation, the beads were washed with lysis buffer and processed for electrophoresis as described above.

For gel-overlay experiments, lysates from control or PMA-treated SKBR3 cells were immunoprecipitated with the 4D5 mAb; samples were separated by SDS/PAGE (6% gels) and the proteins were transferred to PVDF membranes. After blocking, 20 μg of GST–Grb2 or 40 μg of GST–Shc were added to the PVDF membranes and incubated for at least 6 h at 4 °C. Membranes were then washed three times with ice-cold wash buffer [10 mM Tris/HCl, pH 7.5, 140 mM NaCl, 0.05% (v/v) Tween-20], followed by incubation with a 1:20000 dilution of an anti-GST polyclonal antibody (generated in rabbits against bacterially produced GST) for 2 h at 4 °C. Detection of the anti-GST antibody with HRP-conjugated secondary antibodies was as described above.

Cell surface biotinylation

SKBR3 cells were washed in Krebs–Ringer Hepes (KRH) buffer (that contained, in mmol/l: NaCl, 140; KCl, 5; $CaCl_2$, 2; $MgSO_4$, 1.2; KH_2PO_4, 1.2; glucose, 6; Hepes, 25, pH 7.4) for 15 min, and then incubated for 25 min in 1 ml of KRH containing 50 μg/ml of NHS-LC-biotin. The media was then discarded and the monolayers were subjected to another round of biotinylation under identical conditions. Thereafter, excess biotinylation reagent was quenched by incubation for 15 min in KRH containing 10 mM glycine. Cell monolayers were then treated with or without PMA in KRH and cell extracts were prepared in lysis buffer and precipitated with avidin-agarose. The precipitated cell samples were resolved by SDS/PAGE (6% gel), transferred to nitrocellulose and probed with streptavidin–HRP followed by chemiluminescent detection.

Tryptic mapping of ErbB2 and p150/p165

Lysates from PMA-treated SKBR3 cells were immunoprecipitated with the 4D5 mAb. The precipitates were washed three times with lysis buffer, twice with PBS, once with distilled water and resuspended in 100 μl of 0.1 M sodium borate, pH 8.8, containing 25 μg of NHS–biotin. Biotinylation proceeded at room temperature for 4 h and was quenched by the addition of 2 μl of 1 M NH_4Cl for 10 min at room temperature. Samples were then separated by SDS/PAGE (6% gels) and the bands corresponding to ErbB2 or p150 were excised and loaded into separate wells of a 25-cm long SDS-polyacrylamide 10–18% gradient gel. Trypsin (30 μg) was added to each well and the gels were run at 100 V until the samples had concentrated in the stacking gel. The current was then stopped and the gel was maintained at 37 °C for 120 min and electrophoresis was then continued at room temperature. Proteins were transferred to PVDF membranes and probed with streptavidin–HRP followed by chemiluminescent detection.

Kinase assays *in vitro*

PMA-treated SKBR3 cells were lysed in the absence of sodium orthovanadate and immunoprecipitated with the 4D5 mAb, as described above, except that the final two washes of the immunoprecipitates were performed with HNTG buffer (50 mM Hepes, pH 7.4, 50 mM NaCl, 0.1% (v/v) Triton X-100, 10% (v/v) glycerol). Two different protocols were used for the kinase reactions *in vitro*. For radioactive detection, the pellet resulting from the immunoprecipitation was resuspended in 30 μl of HNTG buffer containing 5 mM $MgCl_2$. The kinase reactions were carried out at 4 °C, started by the addition of 15 μM ATP and 3.3 μCi [γ-^{32}P]ATP and terminated at various times by the addition of boiling electrophoresis sample buffer. The samples were separated by SDS/PAGE (6% gels) and analysed by autoradiography or digital PhosphorImaging. The second protocol, aimed at the specific and highly sensitive detection of tyrosine-phosphorylated proteins, was carried out as described above, except that the radioactive ATP was omitted and $MgCl_2$ and ATP were added at 15 mM and 50 μM respectively. Tyrosine-phosphorylated proteins were detected by Western blotting with the 4G10 antibody.

RESULTS

Lower molecular-mass forms of ErbB2 in breast cancer cells

The cleavage of the ectodomain of several receptor tyrosine kinases results in both the release of soluble forms of the ectodomain and the generation of cell-bound truncated fragments [19,23,26–28]. The truncated fragments, that contain the tyrosine kinase domain, may associate with signalling molecules and act as constitutively active receptor forms [21,23]. As sErbB2 has been detected in the culture media of breast cancer cells, we investigated (i) whether accumulation of sErbB2 resulted from PKC-mediated cleavage of the holoreceptor, as occurs in the case of ErbB4 [19]; and (ii) if cleavage of the holoreceptor resulted in the accumulation of cell-bound truncated fragments with signalling capability.

As previously reported [13–15,17], sErbB2 ectodomain could be detected in the conditioned culture media of SKBR3 and BT474 breast cancer cell lines (Figure 1A). The sErbB2 migrated as a diffuse band with an apparent molecular mass of 100–110 kDa; and its release was more efficient in SKBR3 than in BT474 cells (Figure 1A). In contrast, soluble forms of the receptor could not be detected in the conditioned media from MCF-7 cells or in PC12 rat pheochromocytoma cells (Figure 1A), in which the complement of ErbB2 receptors is much lower (Figure 1D, and results not shown). Pulse–chase analysis of metabolically labelled SKBR3 cells showed that sErbB2 slowly accumulated in the culture media of these cells (Figure 1B), and this accumulation was unaffected by PMA (Figure 1C), a PKC-activating treatment that induces cleavage of other receptor

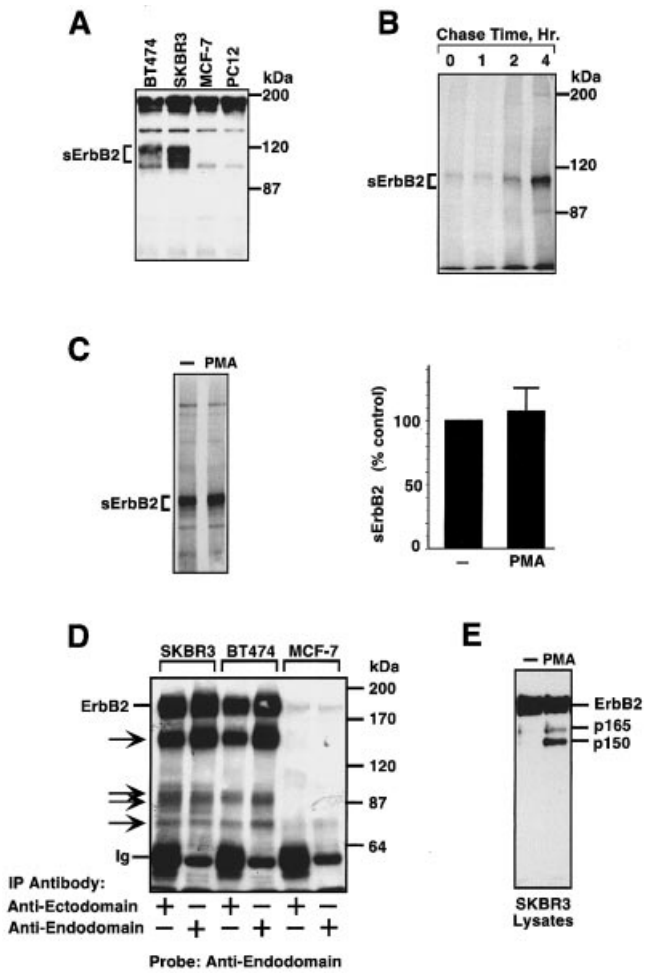

Figure 1 Cell-bound and sErbB2

(**A**) Conditioned media from SKBR3, BT474, MCF-7 and PC12 cells were subjected to immunoprecipitation and Western-blot analysis with the anti-ectodomain antibody 4D5. The molecular-mass markers (kDa) are shown on the right. (**B**) Pulse–chase analysis of sErbB2 generation by SKBR3 cells. Cells were labelled for 16 h with ^{35}S-labelled amino acids, radioactive medium was removed and replaced with complete medium. At the indicated times (h), the culture supernatants were immunoprecipitated with the anti-ectodomain antibody 4D5. Gels were dried and exposed to autoradiographic film. (**C**) Radioactively labelled SKBR3 cells were chased for 4 h in the absence or presence of PMA (1 μM) and exposed to autoradiographic film (left panel) or a digitally-compatible autoradiographic screen for quantification (right panel; means $\pm$ S.E.M. of four different experiments). (**D**) Cell-bound forms of ErbB2. Cell lysates (1 mg) were immunoprecipitated with antibodies recognizing the ectodomain (4D5) or the endodomain (Ab-3) of ErbB2, and analysed by Western blot with the Ab-3 antibody. The arrows indicate lower molecular-mass forms of ErbB2. Ig, immunoglobulin heavy chain. (**E**) Effect of PMA on the amount of cell-associated forms of ErbB2. SKBR3 cells treated with or without PMA for 4 h were lysed and cell lysates (50 μg) were analysed by Western blotting with the Ab-3 antibody. In addition to the holoreceptor (ErbB2), two lower molecular-mass bands (p150 and p165) were identified in cells treated with PMA.

tyrosine kinases [23,26,28] including ErbB4 [19]. This result indicates that ErbB2 solubilization occurs by a mechanism distinct from the one involved in ErbB4 ectodomain cleavage.

To explore whether breast cancer cells contained detectable amounts of truncated lower molecular-mass forms of ErbB2, lysates from SKBR3, BT474 and MCF-7 cells were immunoprecipitated with the 4D5 anti-ectodomain mAb or with the Ab-3 anti-endodomain antibody, and blots were probed with the Ab-3 antibody. In these cell lines, both antibodies immunoprecipitated a 185 kDa protein that corresponded to the ErbB2 holoreceptor (Figure 1D). In addition, in cells overexpressing ErbB2, multiple lower molecular-mass bands were identified by the Ab-3 mAb (Figure 1D, arrows); in particular bands migrating in two regions; one close to the holoreceptor p185^{ErbB2}, and another in the 80–90 kDa segment. On higher resolution gels, the diffuse band migrating close to ErbB2 was split into two forms of 150 and 165 kDa (p150 and p165, see below). These lower molecular-mass forms of ErbB2 were also immunoprecipitated by the anti-ectodomain antibodies MGR2 and Ab-2, and by the anti-endodomain antibodies M6 and Ab-1 (results not shown). The fact that these lower molecular-mass bands were immunoprecipitated by different anti-ErbB2 antibodies, and reacted with the anti-endodomain antibody, together with competition experiments with the peptide against which the Ab-3 antibody was raised (results not shown), indicated that these bands were related to ErbB2, representing cell-associated lower molecular-mass forms of the receptor.

PKC activation induces accumulation of lower molecular-mass forms of ErbB2

To analyse if the presence of the lower molecular-mass forms of ErbB2 could be regulated by PKC, SKBR3 cells were treated with PMA and cell lysates were subjected to Western-blot analysis using the Ab-3 antibody. As shown in Figure 1(E), PMA treatment increased the presence of some of these bands, particularly those that migrated close to the receptor. Although both p150 and p165 increased in SKBR3 cells treated with PMA, the effect of the phorbol ester was quantitatively more pronounced with respect to p150 levels. The bands in the 80–90 kDa region, which could correspond to receptor fragments derived from ErbB2 juxtamembrane cleavage, did not significantly increase in cells treated with PMA (Figure 1E, and results not shown).

The effect of phorbol esters on the generation of these ErbB2 forms was dose- and time-dependent (Figure 2). Half-maximal effect of PMA was observed between 5–10 nM, and full effect was seen at doses above 50 nM (Figure 2A and 2B). In time-course experiments aimed at defining the kinetics of p150/p165 up-regulation, an increase in p165 was detectable at 5 min of treatment with PMA and its amount increased for up to 6 h of treatment and decreased thereafter. The kinetics of the PMA-induced increase in p150 were slower than for p165, with a detectable effect between 30 and 60 min of treatment and a peak at 6 h (Figure 2C and 2D).

In addition to an initial burst in PKC activity, prolonged treatment with phorbol esters is known to induce PKC down-regulation [29]. Since p150/p165 peaked at relatively distant times from the beginning of the PMA treatment, it was of interest to elucidate whether p150/p165 increases were due to PKC activation or instead represented an effect of phorbol esters on PKC down-regulation. Western-blot analysis of phorbol-ester-responsive PKC isoenzymes showed that SKBR3 cells expressed PKCα, PKCγ, PKCδ and PKCϵ (Figure 2E), but expressed very low levels of PKCβ, and PKCθ (results not shown). PMA treatment did not significantly affect PKCϵ amounts, but induced a decrease in PKCα and PKCγ. PKCδ levels were also down-regulated, although to a lesser extent than PKCα or PKCγ. All PKC isoenzymes analysed were present at significant levels at times (3–6 h, Figure 2E) of maximal PMA-induced p150/p165 increases. In other set of experiments, the effect of the PKC inhibitors BIM (Figure 2F) or Gö6983 (Figure 2G) on PMA-induced p150/p165 increases was evaluated. A short pretreatment with these inhibitors prevented the increase in p150/p165 induced by PMA.

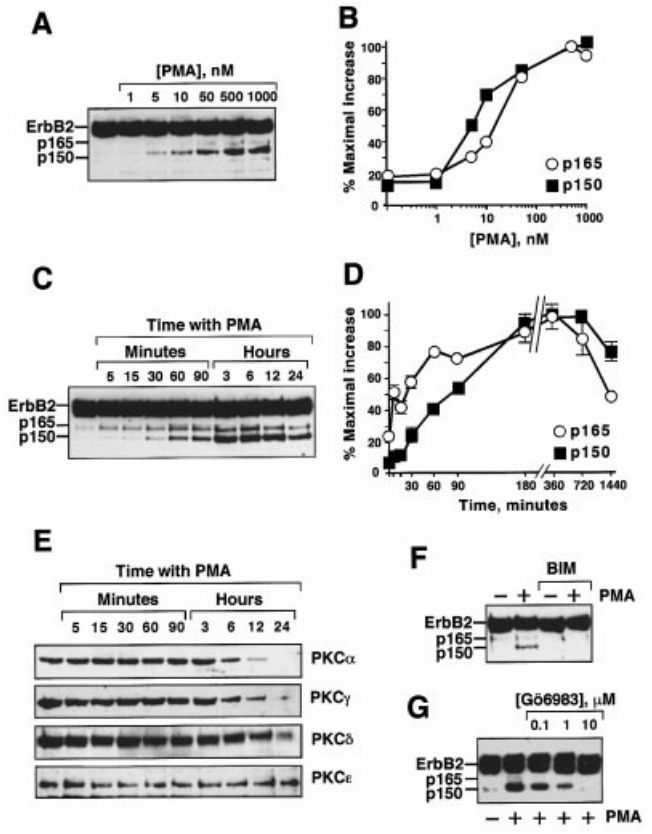

Figure 2 Characterization of the PMA-induced accumulation of lower molecular-mass forms of ErbB2

(**A**) and (**B**) Dose–response of the effect of PMA on the accumulation of p150/p165. SKBR3 cells were treated for 4 h with the indicated concentrations of PMA and the cell lysates (25 μg) analysed by Western blotting with the Ab-3 antibody. (**C**) and (**D**), Time-course analysis of the generation of p150/p165 in response to 1 μM PMA. SKBR3 cells were treated with PMA (1 μM) for the indicated times and lysates (100 μg) were analysed by Western blotting with the Ab-3 antibody. The results shown in (**D**) represent the means $\pm$ S.E.M. of three experiments. (**E**) Expression of different PKC isoenzymes in SKBR3 cells and the effect of PMA on their levels. Cells were treated as in (**C**) and Western blots were analysed with the indicated anti-PKC antibodies. (**F**) and (**G**) Effect of PKC inhibitors on resting and PMA-induced p150/p165 levels. SKBR3 cells were preincubated with 10 μM BIM or with the indicated Gö6983 concentrations for 30 min before addition of 1 μM PMA. Incubations proceeded for 4 h, after which cells were lysed and analysed for p150/p165 levels with the Ab-3 antibody.

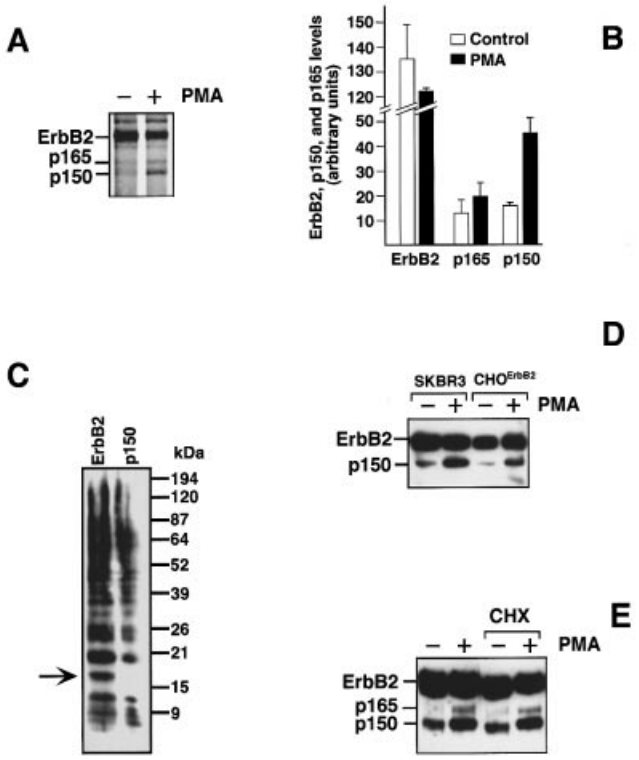

Figure 3 Increases in p150/p165 as a result of ErbB2 cleavage

(**A**) SKBR3 cells were metabolically labelled with 500 μCi/ml of a [^{35}S]methionine/[^{35}S]cysteine mixture for 12 h and chased for 4 h in non-radioactive incubation medium either in the presence or absence of 1 μM PMA. Cell lysates were immunoprecipitated with the 4D5 antibody and immunoprecipitates were analysed by SDS/PAGE and autoradiography. (**B**) Quantification of the effect of PMA on p150/p165 levels from radioactively labelled SKBR3 cells. The data shown represent the means $\pm$ S.E.M. of three experiments. (**C**) Tryptic mapping of ErbB2 and p150. Lysates from SKBR3 cells treated with PMA were immunoprecipitated with the 4D5 mAb and biotinylated as described in the Materials and methods section. Samples were separated by SDS/PAGE (6% gels) and the regions of the gel corresponding to ErbB2 and p150 were excised and loaded, together with trypsin, into the wells of a 10–18% polyacrylamide gel. Digestion with the enzyme proceeded in the stacking gel. Biotinylated peptides were visualized with streptavidin–HRP after blotting of the peptides to PVDF membranes. The arrow indicates a peptide present in the ErbB2 tryptic digest, but absent in the p150 digest. (**D**) Cleavage of ErbB2 in transfected CHO cells. CHO cells transfected with the human ErbB2 cDNA were incubated with PMA for 4 h and cell lysates were analysed by Western blotting with the Ab-3 antibody for the presence of p150/p165. (**E**) Effect of cycloheximide (CHX) on p150/p165 levels. Where indicated, SKBR3 cells were preincubated with 50 μM cycloheximide for 60 min before PMA addition, and the incubations were continued for a further 4 h. Cell lysates were analysed for p150/p165 levels with the Ab-3 antibody.

p150/p165 are generated by N-terminal cleavage of ErbB2

To investigate whether p150/p165 ErbB2 forms were derived from the holoreceptor by truncation, or reflected an effect of phorbol esters on newly-synthesized ErbB2, metabolically labelled SKBR3 cells were chased for 4 h in the absence or presence of PMA. As shown in Figure 3(A), treatment with the phorbol ester induced an increase in p150 and, to a lesser extent, of p165. In addition to the changes in p150/p165, PhosphorImager quantification of data from several different experiments indicated a decrease in the amount of the holoreceptor in PMA-treated cells (Figure 3B). Tryptic mapping of ErbB2 and p150 showed a high degree of overlapping peptide fragments between ErbB2 and p150, with the exception of a fragment that migrated in the 15–21 kDa region (arrow in Figure 3C). The above data, typical of a precursor/product relationship, pointed to proteolytic cleavage as the mechanism of generation of p150/p165.

Phorbol ester-induced increases in p150/p165 were also detected in CHO cells transfected with human cDNA coding for ErbB2 (CHO^{ErbB2}, Figure 3D), and in cycloheximide-treated SKBR3 cells (Figure 3E), further supporting that generation of these lower molecular-mass forms of ErbB2 occurred by proteolytic cleavage. In addition, the data obtained in cycloheximide-treated cells suggests that ErbB2 cleavage was due to stimulation of the activity of the responsible protease, rather than increased expression of the protease in response to PKC activation.

p150/p165 co-exist with p185^{ErbB2} at the plasma membrane, and their generation is independent of classical protein-degradation proteolytic systems

Phorbol esters have been shown to induce internalization and degradation of several receptor tyrosine kinases by directing the

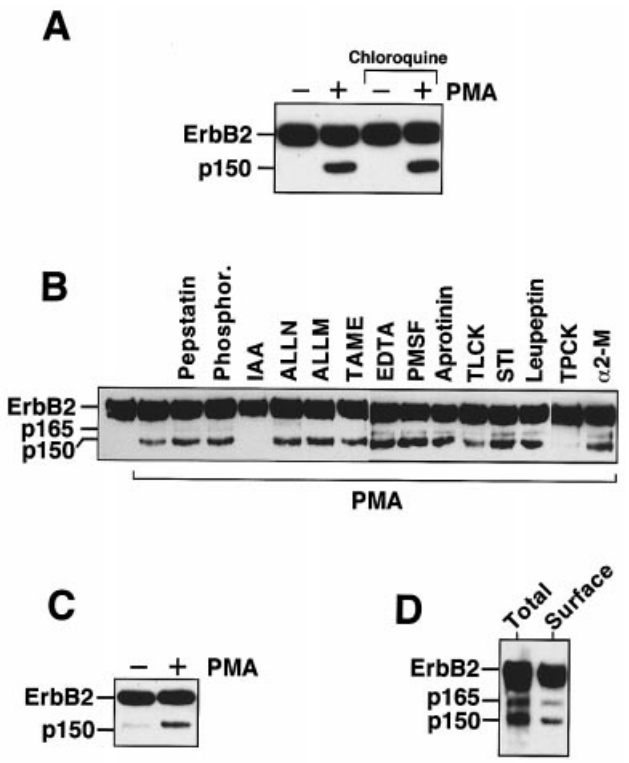

Figure 4 Effect of inhibitors of cellular proteolytic systems on PMA-induced ErbB2 cleavage

(**A**) Effect of the lysosomotropic agent chloroquine on PMA-induced ErbB2 cleavage. Chloroquine (100 μM) was added to SKBR3 monolayers for 30 min before the addition of PMA for 4 h, and cell lysates were tested for the generation of p150/p165 by Western blotting with the Ab-3 antibody. (**B**) Effect of different protease inhibitors on PMA-induced increase in p150/p165 levels. SKBR3 cells were preincubated with the indicated inhibitors for 30 min before PMA addition. The final inhibitor concentrations were: pepstatin, 1 μg/ml; phosphoramidon (Phosphor.), 50 μM; iodoacetic acid (IAA), 100 μM; ALLN, 50 μM; *N*-Ac-Leu-Leu-methioninal (ALLM), 50 μM; N^{α}-*p*-tosyl-L-arginine methyl ester (TAME), 3 mM; EDTA, 10 mM; PMSF, 2 mM; aprotinin, 10 μg/ml; TLCK, 100 μM; soybean trypsin inhibitor (STI), 10 μg/ml; leupeptin, 40 μg/ml; TPCK, 50 μM; α2-macroglobulin (α2-M), 50 μg/ml. (**C**) Surface biotinylation of SKBR3 cells. SKBR3 cells were biotinylated with NHS-LC–biotin and then treated with or without PMA for 4 h. Cell lysates were prepared and precipitated with avidin–Sepharose. The precipitates were electrophoresed on 6% acrylamide gels and ErbB2-related proteins identified by Western blotting with the Ab-3 antibody. (**D**) SKBR3 cells were exposed to 1 μg of the 4D5 mAb at 4 °C for 2 h and excess antibody was eliminated by washing with PBS. Cells were then lysed and surface-bound antibody was isolated by Protein A–Sepharose. ErbB2-related proteins were identified by Western blotting with the Ab-3 antibody.

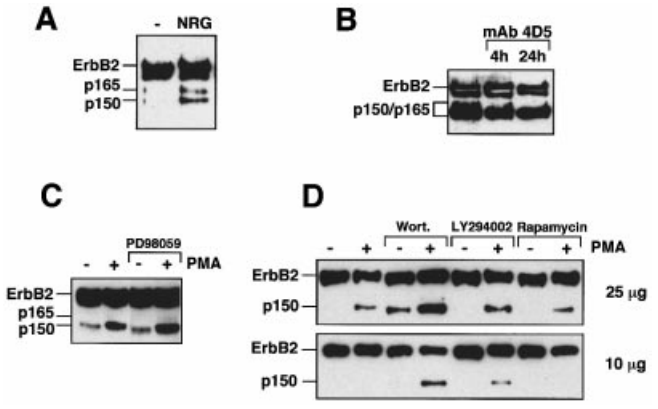

Figure 5 Multiple systems regulate ErbB2 cleavage

(**A**) Effect of the ErbB agonist NRG on p150/p165 levels. NRG (5 nM) was added for 4 h to SKBR3 cells and lysates were prepared for Western-blot analysis with the Ab-3 antibody. (**B**) Effect of the 4D5 antibody *in vivo* on p150/p165 levels. SKBR3 cells were incubated with 10 nM 4D5 for the indicated times, and equal amounts of cell lysates (100 μg) were immunoprecipitated and analysed for p150/p165 levels with the Ab-3 antibody. (**C**) Effect of a MEK inhibitor on PMA-induced p150/p165 levels. PD98059 (50 μM) was preincubated with SKBR3 for 30 min before addition of PMA. Cells were then incubated with the indicated treatments for 4 h, lysed and analysed for p150/p165 levels with the Ab-3 antibody. (**D**) Effect of PI3K and $p70^{s6k}$ inhibitors on PMA-induced increases in p150/p165 levels. The PI3K inhibitors wortmannin (Wort., 100 nM) or LY294002 (20 μM), or the $p70^{s6k}$ inhibitor rapamycin (100 nM) were preincubated with SKBR3 cells for 30 min before addition of PMA; the incubations continued for a further 4 h. Cell lysates (10 μg or 25 μg) were analysed for p150/p165 levels by Western blotting with the Ab-3 antibody.

receptors to lysosomes [30,31]. To investigate whether p150/p165 were intermediates generated during lysosome-mediated degradation of the holoreceptor, we analysed the effect of PMA in the presence of inhibitors of lysosomal proteases, such as chloroquine and leupeptin [32]. Pretreatment with these inhibitors was unable to prevent PMA-induced increases in the N-terminal ErbB2 cell-associated fragments (Figure 4A and 4B). Analogously, pre-incubation of SKBR3 cells with the proteasome inhibitor *N*-Ac-leu-leu-norleucinal (ALLN) did not affect phorbol ester-induced increases in p150/p165 (Figure 4B).

In addition to lysosomal and proteasomal pathways, proteolytic cleavage of receptor tyrosine kinases may also occur during transit of the receptors from intracellular sorting compartments to the plasma membrane. To explore whether cleavage of ErbB2 occurred during its intracellular transit before the receptor reached the cell surface, or whether mature receptor already present at the surface was susceptible to proteolytic cleavage, SKBR3 cells were surface-biotinylated at 4 °C and then treated with PMA at 37 °C. Under resting conditions the major biotinylated form of ErbB2 corresponded to the holoreceptor; treatment with PMA induced the appearance of biotin-labelled p150 (Figure 4C). In addition, selective cell-surface immunoprecipitation experiments showed that the truncated p150/p165 forms of ErbB2 were exposed at the surface of the cell (Figure 4D), indicating that p150/p165 and the $p185^{ErbB2}$ holoreceptor co-exist at the plasma membrane.

Taken together, the above data indicated that cleavage of the $p185^{ErbB2}$ holoreceptor occurred by a mechanism that was independent of classical protein maturation or degradation proteases and pointed to the plasma membrane as a potential site for the attack of the holoreceptor by protease(s). Based on this, and to gain insights into the proteolytic activities involved in the cleavage of ErbB2, we treated SKBR3 cells with a panel of inhibitors that target the different protease families. From this screening we identified two, iodoacetic acid and tosylphenylalanylchloromethyl ketone (TPCK), that efficiently neutralized PMA-induced cleavage of ErbB2 (Figure 4B). The hydroxamic acid-based inhibitor TAPI-2, that blocks the regulated release of several membrane-bound proteins [33], was unable to prevent the regulated cleavage of ErbB2 (results not shown).

Multiple mechanisms regulate p150/p165 levels

To further advance the knowledge of the mechanisms that regulate p150/p165 generation, we investigated the effect of several treatments that affect ErbB2 signalling. First, treatments that target the ectodomain of ErbB2 and have opposite effects on ErbB2 signalling were analysed. As shown in Figure 5(A),

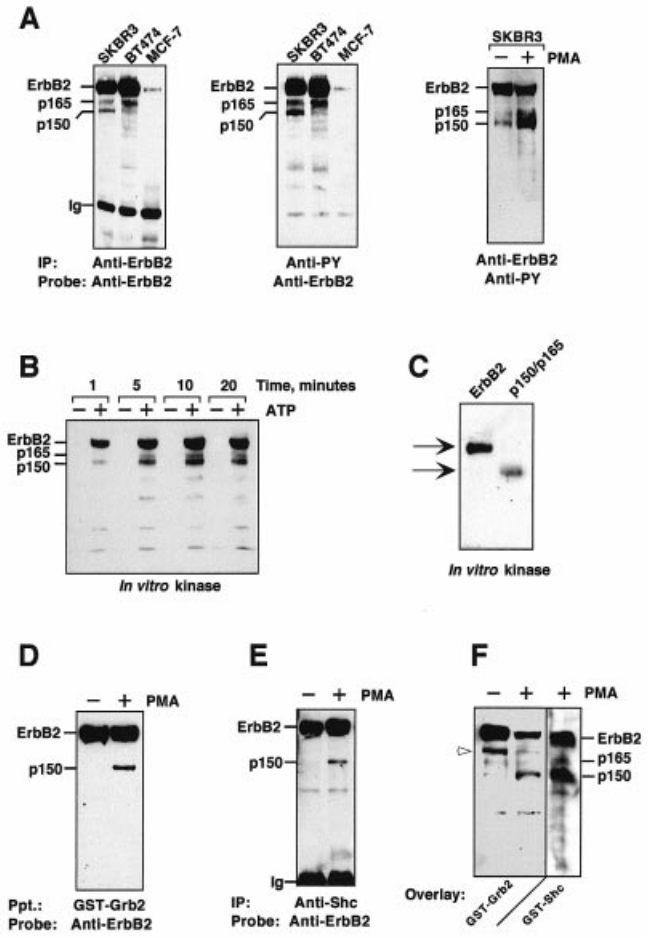

Figure 6 p150/p165 are tyrosine-phosphorylated and associated with signalling molecules

(**A**) SKBR3, BT474 or MCF-7 lysates (1 mg) were immunoprecipitated with the Ab-3 anti-endodomain antibody (left panel) or with the anti-phosphotyrosine antibody 4G10 (centre panel) and the blots were probed with the Ab-3 antibody. The right panel shows the phosphotyrosine content of ErbB2 and the related p150/p165 fragments in SKBR3 cells treated with or without PMA for 4 h. The samples (1 mg) were immunoprecipitated with the 4D5 mAb followed by Western blotting with anti-phosphotyrosine antibodies. (**B**) *In vitro* kinase activity of 4D5 immunoprecipitates from PMA-treated SKBR3 cells. Where indicated, the immunoprecipitates (from a 100-mm dish, divided into eight different tubes) were incubated in the absence (−) or presence (+) of exogenously added 50 μM ATP and the reactions were allowed to proceed at room temperature for the times shown. After SDS/PAGE, the tyrosine-phosphorylated proteins were identified by Western blotting with anti-phosphotyrosine antibodies. (**C**) *In vitro* kinase activity of isolated ErbB2 and p150/p165. Lysates from PMA-treated SKBR3 cells were immunoprecipitated with the 4D5 mAb, and separated by SDS/PAGE (6% gel). The gel was sliced and those pieces corresponding to ErbB2 and p150/p165 were electroeluted and assayed for kinase activity as described in the Materials and methods section. (**D**) Dishes (100-mm) of SKBR3 cells were incubated in the absence or presence of PMA (1 μM) for 4 h and the lysate from each dish (2 mg) was precipitated for 2 h with 10 μg of GST–Grb2 coupled to GSH-agarose beads. The precipitated proteins were separated by SDS/PAGE (6% gel) and after transfer to PVDF membranes, the ErbB2-related proteins were recognized by the Ab-3 antibody. (**E**) Association of p150 and the $p185^{ErbB2}$ holoreceptor to Shc. SKBR3 cells were treated with PMA (1 μM, 4 h) and lysates from 100-mm dishes were precipitated with 5 μg of anti-Shc antiserum. The precipitated proteins were separated by SDS/PAGE (6% gel), and the ErbB2-related proteins were identified with the Ab-3 antibody. (**F**) Direct association of Shc and Grb2 with ErbB2 and the p150/p165 fragments. Lysates from control or PMA-treated SKBR3 cells were immunoprecipitated with the 4D5 antibody and ErbB2 and the p150/p165 fragments were separated by SDS/PAGE. GST-Grb2 or GST-Shc were then added, followed by detection of the GST module by anti-GST antibodies. A band that co-immunoprecipitated with ErbB2 and was recognized by Grb2 (but failed to be recognized by the anti-ErbB2 Ab-3 mAb, results not shown) is indicated by an open arrowhead.

treatment with the ErbB agonist NRG induced an increase in p150/p165 that was qualitatively similar to that induced by PMA treatment, but of lower magnitude (results not shown). On the other hand, long-term treatment of SKBR3 cells with the mAb 4D5, which inhibits NRG action and causes down regulation of ErbB2 [34], resulted in the opposite effect, i.e. decreased p150/p165 levels (Figure 5B).

Since NRG induced a significant increase in p150/p165 levels, it was therefore likely that signal transduction pathways triggered upon activation of ErbB receptors were involved in the regulation of the N-terminal cleavages that affected this receptor. The mitogen-activated protein kinase (MAPK) pathway is activated upon ErbB2 stimulation, and signalling by this receptor is accompanied by a significant increase in MAPK activity [35]. In addition, the MAPK pathway is a target for several PKC-induced intracellular events, because of the action of PKC on the MAPK upstream-activator kinases [36]. To elucidate whether this intracellular pathway was implicated in the regulation of p150/p165 levels, we tested the effect of PD98059 (an inhibitor of MAPK kinase (MEK), the kinase that phosphorylates and activates the MAPK, Erk1 and Erk2 [36,37]) on resting and PMA-induced p150/p165 levels. Pretreatment with this inhibitor, however, did not affect the PKC-mediated cleavage of ErbB2 (Figure 5C), even though it efficiently blocked PMA-induced MAPK activation (results not shown). These results indicate that the MAPK pathway does not act as an intermediate in the action of PKC on ErbB2 cleavage. In contrast, wortmannin, which inhibits PI3K [38], had a significant effect on p150/p165 levels (Figure 5D). This inhibitor induced an increase in resting p150 levels (Figure 5D, upper panel), and strongly potentiated PMA-induced p150/p165 increases. Analogous results were obtained with the unrelated PI3K inhibitor LY294002 (Figure 5D). Rapamycin, which inhibits $p70^{s6k}$, a downstream target of PI3K [38], did not affect either resting or PMA-induced increases in p150/p165, thus excluding the participation of the $p70^{s6k}$ pathway in the regulatory action of PI3K on ErbB2 truncation.

p150/p165 are tyrosine-phosphorylated and associate with signalling molecules

As an initial step towards the evaluation of the functional properties of p150/p165, their tyrosine phosphorylation and association with signalling intermediates were investigated. Probing Western blots of anti-phosphotyrosine immunoprecipitates from SKBR3 or BT474 cells with the anti-ErbB2 endodomain antibody showed that, in addition to the holoreceptor, the lower molecular-mass fragments of 150 and 165 kDa were also tyrosine-phophorylated (Figure 6A, centre panel). Other tyrosine-phosphorylated proteins were also detected in the 80–90 kDa region, but with a less marked phosphotyrosine content than p150/p165. Direct evidence that p150/p165 were tyrosine-phosphorylated was verified by immunoprecipitation of control and PMA-treated SKBR3 cell lysates with the anti-ErbB2 antibody followed by probing of Western blots with the anti-phosphotyrosine antibody (Figure 6A, right panel). Immunoprecipitation and Western blotting with the anti-phosphotyrosine antibody indicated that $p185^{ErbB2}$, p150 and p165 were the most abundantly tyrosine-phosphorylated proteins in whole lysates from SKBR3 and BT474 cells (results not shown). In MCF-7 cells, and using similar exposure times, traces of tyrosine phosphorylation were evident in the holoreceptor only (Figure 6A).

Kinase reactions *in vitro* were performed to explore whether p150/p165 were active kinases. To specifically measure tyrosine

phosphorylation of ErbB2 or p150/p165 substrates, lysates from PMA-treated SKBR3 cells were prepared in the absence of phosphatase inhibitors and immunoprecipitated with the 4D5 mAb. The immunoprecipitates were subjected to kinase reactions *in vitro* in the absence or presence of ATP, and tyrosine-phosphorylated proteins were detected in Western blots with the anti-phosphotyrosine mAb. As shown in Figure 6(B), tyrosine phosphorylation of ErbB2, p150/p165, as well as of several other low molecular-mass peptides increased with time, but only in samples containing exogenously added ATP. Phosphorylation *in vitro* of ErbB2, p150 and p165 was also verified by carrying out the reactions in the presence of [γ-^{32}P]ATP, followed by SDS/PAGE and autoradiographic analysis (results not shown). To investigate whether ErbB2 or p150/p165 themselves had kinase activity, 4D5 immunoprecipitates from PMA-treated SKBR3 cells were subjected to SDS/PAGE (6% gel) followed by excision of the regions of the gel corresponding to ErbB2 or p150/p165 and electroelution of the bands from the gel fragments. The eluted material was immunoprecipitated with the 4D5 antibody and then kinase reactions were performed *in vitro*. As shown in Figure 6(C), ErbB2 and p150/p165 were readily autophosphorylated in these assays, indicating that p150/p165 had intrinsic kinase activity.

In PMA-stimulated SKBR3 cells, immunoprecipitation with an antibody against the adapter molecule Shc, followed by Western-blot analysis with the anti-endodomain antibody Ab-3 indicated that in addition to the p185^{ErbB2} holoreceptor, p150 could also co-precipitate with Shc (Figure 6E). Precipitation with a GST–Grb2 fusion protein indicated that p150 was also able to interact with Grb2 (Figure 6D). Gel overlay experiments using GST–Shc or GST–Grb2 to probe blots from 4D5 immunoprecipitates demonstrated that the interaction of these signalling intermediates to p150/p165 was direct (Figure 6F). Thus the truncated forms of ErbB2 may associate with signalling molecules that participate in the ErbB signalling network.

DISCUSSION

Release of soluble forms of the ectodomain of receptor tyrosine kinases may occur by genetic or proteolytic mechanisms [23]. In the latter case, cleavage of the receptor also results in the generation of cell-associated truncated forms containing the tyrosine kinase domain of the receptor. These cell-bound forms may be constitutively active and, in this respect, proteolytic cleavage has been postulated to act as a natural cellular activating mechanism [19,23]. Since the soluble ectodomain of ErbB2 has been detected in the culture supernatants of cancer cells [13,14,17], and in the body fluids from animals [16] and humans with advanced breast cancer [15], we decided to investigate if, as a result of holoreceptor cleavage, cancer cells expressed signalling-competent truncated forms of ErbB2. In the present report, the presence, mechanism of generation, regulating pathways and signalling properties of truncated cell-associated forms of ErbB2 are described.

The ectodomain of ErbB2 has been detected in a soluble form from the culture media of breast cancer cells [13,14,17], and the mechanism of generation of this truncated form may involve proteolytic cleavage of the holoreceptor [13–15]. Cleavage of the ectodomain of several transmembrane proteins, including ErbB4 [19], can be regulated by treatments that result in increased PKC activity [39,40]. The truncation of ErbB4 [19] and other sensitive proteins occurs at a juxtamembrane site, thus releasing most of their ectodomain [39,41]. Because activation of PKC can induce accumulation of sErbB4 [19] and sErbB2 [14] ectodomains in the culture media of cells expressing these receptors, it was of interest to investigate if the mechanism for the solubilization of both receptors was the same. In SKBR3 cells, pulse–chase experiments indicated that the release of soluble ErbB2 was a slow process, unresponsive to PKC activation. This is in line with recent data obtained in BT474 cells, in which release of sErbB2 ectodomain was up regulated by PKC activators, but only after chronic exposure to phorbol esters [42]. Therefore the protease(s) involved in the cleavage of the ectodomain of ErbB2 may be unrelated to the proteases that act in the regulated release of the ectodomain of ErbB4, and in this respect shedding of the sErbB2 could be due to the activity of a novel group of membrane-protein ectodomain cleaving enzymes.

Cleavage of the ectodomain of p185^{ErbB2} in a juxtamembrane region should result in the generation of two fragments: a soluble ectodomain of 100–110 kDa, and a cell-bound fragment of approximately 80–90 kDa. Analysis of cell lysates from SKBR3 and BT474 cells revealed, in addition to the holoreceptor, a heterogeneous pattern of proteins that were recognized by an antibody raised to the C-terminus of ErbB2. Immunoprecipitation of extracts from these cell lines with antibodies directed towards different domains of the ErbB2 receptor indicated that these proteins were related to ErbB2. Some immunoreactive bands were detected in an 80–90 kDa region, but the most prominent ErbB2-related proteins migrated with molecular masses of 150 and 165 kDa.

Analogously to the truncated forms that arise by cleavage in a juxtamembrane position in several transmembrane proteins [40], the amount of p150 and p165 forms of ErbB2 was also up-regulated by treatments that stimulate the activity of PKC. Studies on the mechanism of generation of these lower molecular-mass forms of ErbB2 indicated that proteolytic cleavage could be responsible for the production of these forms. Strong evidence, pointing in this direction, was obtained by pulse–chase analysis, which revealed increased levels of p150 in cells treated with PMA, whereas the amount of the holoreceptor decreased; by tryptic-peptide mapping of ErbB2 compared with p150/p165, and by cell surface biotinylation experiments. In addition, in SKBR3 cells treated with the protein synthesis inhibitor cycloheximide, and in CHO cells transfected with human ErbB2, PMA was still able to increase the levels of p150/p165, indicating that these lower molecular-mass forms were not biosynthetic intermediates but were derived from the holoreceptor.

Even though PKC may also regulate the cleavage of the ectodomain of several transmembrane proteins, including some receptor tyrosine kinases, important differences exist between this type of cleavage and the one that affects the N-terminus of ErbB2. First, the kinetics of generation of truncated N-terminal forms of ErbB2 were much slower, peaking several hours after treatment with PMA, whereas PMA-induced cleavage at a juxtamembrane position of several membrane-bound proteins, such as proTGFα [43] and TrkA [23], was much faster ($t_{1/2}$ = 5–15 min). The delayed time course of the generation of the truncated forms of ErbB2 also raised the question of whether the effect of PMA was due to down-regulation of PKC, rather than activation. However, measurement of different PKC isoforms by Western blotting, together with experiments in which well-known PKC inhibitors were used, clearly indicated that the effect of phorbol esters on ErbB2 cleavage was due to PKC activation. Another substantial difference between PMA-induced ErbB2 N-terminal cleavage and the regulated cleavage of proteins at their juxtamembrane region was the sensitivity of cleavage to different protease inhibitors. TAPI-2, a hydroxamic acid-based inhibitor of metalloproteases, that efficiently blocks PMA-induced ectodomain shedding of several transmembrane proteins [33] was, however, inefficient in preventing p150/p165 generation.

In contrast, p150/p165 generation was largely inhibited by TPCK and iodoacetic acid. Since TPCK targets serine proteases, the data with this reagent indicate that a serine protease acts in the N-terminal cleavage of ErbB2. The data with iodoacetic acid support the observation that the cleavage process was sensitive to thiol-group alterations; whether this drug affects the structure of the protease, the substrate or an intermediate component is unknown.

In addition to PKC, other signalling pathways regulated the generation of ErbB2 truncated forms. NRG, which binds ErbB2 with a very low affinity [22] but stimulates its tyrosine phosphorylation when co-expressed with ErbB3 or ErbB4 [22], increased p150/p165 generation, although to a lesser extent than PKC activators. On the other hand, the mAb 4D5 was able to slightly, but reproducibly, down-regulate the amount of truncated forms of ErbB2. Treatment with this mAb has been shown to reduce the amount of the ErbB2 holoreceptor in breast cancer cell lines [44]. Whether the mAb 4D5 effect is due to direct down-regulation of p150/p165 or to an indirect effect caused by a decrease in the holoreceptor remains to be investigated.

By using inhibitors of several intracellular pathways, we evaluated the participation of other kinase activities in p150/p165 generation. The MAPK inhibitor PD98059 [37] was unable to significantly affect either resting or PMA-induced levels of p150/p165, thus excluding the participation of the MAPK pathway in the action of phorbol esters. Treatment of SKBR3 cells with the PI3K inhibitors wortmannin and LY294002 increased p150/p165 generation, and potentiated the increase in these truncated forms induced by PKC activation, indicating that PI3K activity may negatively regulate the generation of these truncated fragments. The effect of PI3K inhibitors on ErbB2 cleavage did not seem to be due to inhibition of ErbB2 down-regulation, thus allowing more substrate (ErbB2) to be attacked by the protease. In fact, even though PI3K may participate in the internalization of several membrane proteins [45], the amount of ErbB2 holoreceptor in cells treated with PI3K inhibitors did not seem to be significantly different from the receptor present in untreated cells. $p70^{s6k}$ is one of the downstream targets of PI3K [38]. Rapamycin, which inhibits the action of $p70^{s6k}$ was, however, ineffective in altering either resting or PMA-induced increase in p150/p165, indicating that the PI3K inhibitors acted through an intracellular pathway independent of $p70^{s6k}$. A conclusion from these data is that cleavage of ErbB2 at the N-terminus is a highly regulated process, controlled by the activity of several intracellular signalling pathways. The participation of protein kinases, such as PKC, in the regulation of this activity suggests that the proteases, or other signalling intermediates, are targets for protein-kinase-induced phosphorylation. A more detailed description of the mechanisms involved in ErbB2 cleavage will require the identification of the components of this proteolytic system.

An important implication of the data reported in the present work, is the fact that truncated forms of ErbB2 may be autonomously active in the absence of ligand. In line with this hypothesis are the data obtained by analysing the signalling state of the truncated N-terminal forms of ErbB2 present in SKBR3 and BT474 breast cancer cells. Immunoprecipitation with anti-phosphotyrosine or anti-ErbB2 antibodies indicated that the truncated fragments of ErbB2 were constitutively phosphorylated on tyrosine residues, suggesting that these truncated forms may act autonomously in the absence of any exogenously added ligand. In support of this hypothesis was the finding that signalling molecules that associate with ErbB2, such as Shc or the adapter protein Grb2, could co-precipitate the truncated forms of ErbB2 in addition to the holoreceptor. Truncated forms of ErbB2 may thus participate in a continuous signalling stimulus, acting alone or in concert with the holoreceptor.

Several indications suggest that N-terminal truncations of ErbB receptors may act as activating mechanisms. First, the genetic evidence obtained from the molecular analysis of an EGFR mutant form found in several different solid tumours, such as glioblastomas, breast and lung cancers [46]. This aberrant EGFR (termed ΔEGFR) lacks 267 amino acids in a region that is located at the N-terminus of the receptor, and this truncation creates a highly tumourigenic mutant receptor [47,48]. Based on the molecular mass of the ErbB2 truncated forms described in the present study, a region very similar to the one lacking in the ΔEGFR is expected to be missing in p150/p165 ErbB2 forms. Secondly, data generated with artificial truncations of the N-terminus of ErbB2 [49,50] also support that the N-terminal region of ErbB receptors may act as a brake for the tyrosine kinase activity present in the endodomain. In the case of ErbB2, p150 and p165, it is not clear whether the truncated forms have an increased activity when compared with the receptor. Preliminary analysis of phosphotyrosine content *in vivo* indicated that the truncated fragments had a higher phosphotyrosine/protein ratio than the parental holoreceptor (results not shown). However, kinase assays *in vitro* have shown comparable amounts of ^{32}P incorporation into p150 and ErbB2, indicating analogous autophosphorylation capabilities.

Physiologically, cleavage of the N-terminus of ErbB2 may represent a natural cellular mechanism of receptor activation in the absence of ligand, or in conditions in which presentation of the ligand to ErbB2 by the other ErbB co-receptors is deficient. Cleavage of ErbB2 may represent a novel mechanism for receptor transactivation, where non-ErbB ligand agonists could stimulate the MAPK pathway through the PKC-mediated proteolytic activation of ErbB2. From the pathological point of view, these activating truncations may, as occurs with the ΔEGFR, contribute to tumour development or progression [46,48], or create resistance to therapy [51]. In the design of therapeutic weapons that target the ErbB family of receptor tyrosine kinases over-expressed in cancer cells, the possible co-expression of these truncated forms should be taken into account in order for the therapy to be highly efficient.

We thank the following scientists for their gifts of reagents: Dr Piero Crespo, Dr Mark X. Sliwkowski, Dr Roy A. Black, Dr Matthias Kraus and Dr John Mendelsohn. We also thank Dr Jorge Moscat for his expert opinions on several aspects of PKC regulation. Finally, we would like to thank the European Community, the Fundación Ramón Areces, and the Spanish Ministry of Education and Culture for financial support.

REFERENCES

1 Burden, S. and Yarden, Y. (1997) Neuron **18**, 847–855
2 Hynes, N. E. and Stern, D. F. (1994) Biochim. Biophys. Acta **1198**, 165–184
3 Tzahar, E. and Yarden, Y. (1998) Biochim. Biophys. Acta **1377**, M25–M37
4 Britsch, S., Li, L., Kirchhoff, S., Theuring, F., Brinkmann, V., Birchmeier, C. and Riethmacher, D. (1998) Genes Dev. **12**, 1825–1836
5 Riethmacher, D., Sonnenberg-Riethmacher, E., Brinkmann, V., Yamaai, T., Lewin, G. R. and Birchmeier, C. (1997) Nature (London) **389**, 725–730
6 Sibilia, M., Steinbach, J. P., Stingl, L., Aguzzi, A. and Wagner, E. F. (1998) EMBO J. **17**, 719–731
7 Scott, G. K., Robles, R., Park, J. W., Montgomery, P. A., Daniel, J., Holmes, W. E., Lee, J., Keller, G. A., Li, W. L., Fendly, B. M. et al. (1993) Mol. Cell. Biol. **13**, 2247–2257
8 Ullrich, A., Coussens, L., Hayflick, J. S., Dull, T. J., Gray, A., Tam, A. W., Lee, J., Yarden, Y., Libermann, T. A., Schlessinger, J. et al. (1984) Nature (London) **309**, 418–425
9 Flickinger, T. W., Maihle, N. J. and Kung, H.-J. (1992) Mol. Cell. Biol. **12**, 883–893
10 Reiter, J. L. and Maihle, N. J. (1996) Nucleic Acids Res. **24**, 4050–4056
11 Katoh, M., Yazaki, Y., Sugimura, T. and Terada, M. (1993) Biochem. Biophys. Res. Commun. **192**, 1189–1197

12 Petch, L. A., Harris, J., Raymond, V. W., Blasband, A., Lee, D. C. and Earp, H. S. (1990) Mol. Cell. Biol. **10**, 2973–2982
13 Lin, Y. J. and Clinton, G. M. (1991) Oncogene **6**, 639–643
14 Zabrecky, J. R., Lam, T., McKenzie, S. J. and Carney, W. (1991) J. Biol. Chem. **266**, 1716–1720
15 Pupa, S. M., Ménard, S., Morelli, D., Pozzi, B., De Palo, G. and Colnaghi, M. I. (1993) Oncogene **8**, 2917–2923
16 Langton, B. C., Crenshaw, M. C., Chao, L. A., Stuart, S. G., Akita, R. W. and Jackson, J. E. (1991) Cancer Res. **51**, 2593–2598
17 Alper, O., Yamaguchi, K., Hitomi, J., Honda, S., Matsushima, T. and Abe, K. (1990) Cell Growth Different. **1**, 591–599
18 Basu, A., Raghunath, M., Bishayee, S. and Das, M. (1989) Mol. Cell. Biol. **9**, 671–677
19 Vecchi, M., Baulida, J. and Carpenter, G. (1996) J. Biol. Chem. **271**, 18989–18995
20 Vecchi, M. and Carpenter, G. (1997) J. Cell Biol. **139**, 995–1003
21 Vecchi, M., Rudolph-Owen, L. A., Brown, C. L., Dempsey, P. J. and Carpenter, G. (1998) J. Biol. Chem. **273**, 20589–20595
22 Tzahar, E., Pinkas-Kramarski, R., Moyer, J. D., Klapper, L. N., Alroy, I., Levkowitz, G., Shelly, M., Henis, S., Eisenstein, M., Ratzkin, B. J. et al. (1997) EMBO J. **16**, 4938–4950
23 Cabrera, N., Díaz-Rodríguez, E., Becker, E., Zanca, D. M. and Pandiella, A. (1996) J. Cell Biol. **132**, 427–436
24 Ausubel, F. M., Brent, R., Kingston, R. E., Moore, D. D., Seidman, J. G., Smith, J. A. and Struhl, K. (1987) Current Protocols in Molecular Biology, John Wiley & Sons, New York
25 Guan, K. L. and Dixon, J. E. (1991) Anal. Biochem. **192**, 262–267
26 Downing, J. R., Roussel, M. F. and Sherr, C. J. (1989) Mol. Cell. Biol. **9**, 2890–2896
27 Prat, M., Crepaldi, T., Gandino, L., Giordano, S., Longati, P. and Comoglio, P. (1991) Mol. Cell. Biol. **11**, 5954–5962
28 Yee, N. S., Hsiau, C.-W., Serve, H., Vosseler, K. and Besmer, P. (1994) J. Biol. Chem. **269**, 31991–31998
29 Mellor, H. and Parker, P. J. (1998) Biochem. J. **332**, 281–292
30 Sorkin, A. and Waters, C. M. (1993) BioEssays **15**, 375–382
31 van der Geer, P., Hunter, T. and Lindberg, R. A. (1994) Annu. Rev. Cell Biol. **10**, 251–337
32 Kornfeld, S. and Mellman, I. (1989) Annu. Rev. Cell Biol. **5**, 483–525
33 Arribas, J., Coodly, L, Vollmer, P., Kishimoto, T. K., Rose-John, S. and Massagué, J. (1996) J. Biol. Chem. **271**, 11376–11382
34 Lewis, G. D., Lofgren, J. A., McMurtrey, A. E., Nuijens, A., Fendly, B. M., Bauer, K. D. and Sliwkowski, M. X. (1996) Cancer Res. **56**, 1457–1465
35 Ben-Levy, R., Paterson, H. F., Marshall, C. J. and Yarden, Y. (1994) EMBO J. **13**, 3302–3311
36 Cohen, P. (1997) Trends Cell Biol. **7**, 353–361
37 Dudley, D. T., Pang, L., Decker, S. J., Bridges, A. J. and Saltiel, A. R. (1995) Proc. Natl. Acad. Sci. U.S.A. **92**, 7686–7689
38 Monfar, M., Lemon, K. P., Grammer, T. C., Cheatham, L., Chung, J., Vlahos, C. J. and Blenis, J. (1995) Mol. Cell. Biol. **15**, 326–337
39 Massagué, J. and Pandiella, A. (1993) Annu. Rev. Biochem. **62**, 515–541
40 Hooper, N. M., Karran, E. H. and Turner, A. J. (1997) Biochem. J. **321**, 265–279
41 Rose-John, S. and Heinrich, P. C. (1994) Biochem. J. **300**, 281–290
42 Christianson, T. A., Doherty, J. K., Lin, Y. J., Ramsey, E. E., Holmes, R., Keenan, E. J. and Clinton, G. M. (1998) Cancer Res. **58**, 5123–5129
43 Pandiella, A. and Massagué, J. (1991) Proc. Natl. Acad. Sci. U.S.A. **88**, 1726–1730
44 Kumar, R., Shepard, H. M. and Mendelsohn, J. (1991) Mol. Cell. Biol. **11**, 979–986
45 Shpetner, H., Joly, M., Hartley, D. and Corvera, S. (1996) J. Cell Biol. **132**, 595–605
46 Nagane, M., Huang, H. J. and Cavenee, W. K. (1997) Curr. Opin. Oncol. **9**, 215–222
47 Nishikawa, R., Ji, X.-D., Harmon, R. C., Lazar, C. S., Gill, G. N., Cavenee, W. K. and Su Huang, H.-J. (1994) Proc. Natl. Acad. Sci. U.S.A. **91**, 7727–7731
48 Huang, H. S., Nagane, M., Klingbeil, C. K., Lin, H., Hishikawa, R., Ji, X. D., Huang, C. M., Gill, G. N., Wiley, H. S. and Cavenee, W. K. (1997) J. Biol. Chem. **272**, 2927–2935
49 Di Fiore, P. P., Pierce, J. H., Kraus, M. H., Segatto, O., King, C. R. and Aaronson, S. A. (1987) Science **237**, 178–182
50 Bargmann, C. I. and Weinberg, R. A. (1988) EMBO J. **7**, 2043–2052
51 Nagane, M., Levitzki, A., Gazit, A., Cavenee, W. K. and Huang, H. J. (1998) Proc. Natl. Acad. Sci. U.S.A. **95**, 5724–5729

Received 7 May 1999/6 August 1999; accepted 20 September 1999